ChemPubSoc Europe

DOI: 10.1002/chem.201402614

CHEMISTRY
A European Journal
Full Paper

Nanoparticles

Confinement of Cu^{II}–Phthalocyanine in a Bioinspired Hybrid Nanoparticle-Assembled Structure Yields Selective and Stable Epoxidation Catalysts

Joydeb Manna, Arlin Jose Amali, and Rohit Kumar Rana*[a]

Abstract: Herein, we demonstrate that a bioinspired assembly of silica nanoparticles with polyamines as structure-directing agents similar to that known for the biosilicification of diatoms can pave the way for the efficient encapsulation of sulfonated copper–phthalocyanine in a hybrid microcapsule structure, in which the organic component provides a capable environment for its catalytic activity in epoxidation reactions and the nanoassembled structure imparts stability.

Introduction

Metalloenzyme-catalyzed oxidation reactions are known to be highly selective and to proceed under very mild conditions. Thus, mimicking enzyme functions is a field of great interest to develop new and very effective biologically inspired catalysts.[1] It has been established that transition-metal complexes of corrole, salen, porphyrins, and phthalocyanines resemble the functionality of cytochrome P450, an extensively studied monooxygenase enzyme.[2] The combination of a metal complex and peroxides as an oxidizing system has been therefore investigated to direct the metal-promoted peroxide cleavage towards the oxidation of hydrocarbons with high selectivity.[3] Particularly inspired by copper-containing enzymes, a variety of synthetic systems that incorporate copper complexes have been studied.[4] However, most of these metal complexes exhibit decreased catalytic activities due to unwanted ligand oxidation or the formation of unactivated complexes. Therefore, the stabilization of the metal complex in a support is imperative for further developments in this field. The rationale for an ideal support matrix would be to make use of a confined space to prevent complex aggregation and to stabilize the complex by providing suitable anchoring sites in the matrix.

In this context, metal–phthalocyanines (MPc) are the most intriguing biomimetic complexes, which have been widely studied in heterogeneous systems by using either porous inorganic solids or polymers as a catalyst support.[5] Parton et al. have shown that encapsulation of FePc in zeolite-Y embedded in polydimethylsiloxane membranes can mimic the functionality of cytochrome P-450.[6] Similarly, encapsulated CuPc, CoPc, and VPc in zeolite-Y have been used for the oxidation of styrene.[7] Physical entrapment of metallophthalocyanines has also been carried out in activated carbon black and silica by using sol–gel processing.[8] The immobilization of CuPc complexes on mesoporous silica has been achieved by using the chemical-vapor-deposition method.[9] The use of molecular sieves as the support has been evaluated as well.[10] The pores or supercages are believed to provide a confined medium for increased catalytic activity and selectivity;[11] however, tedious preparation steps are often required to synthesize the metal complexes inside the cages especially for complexes larger than the pore sizes of the zeolites. Moreover, constraining a rather flexible metal complex in a rigid matrix can sometime result in complex distortion and even incomplete coordination.

Covalent grafting of metallophthalocyanines onto silica materials or onto organic polymers presents another possible approach.[12] Recently, it has been demonstrated that Pc conjugated with a protein matrix of serum albumins can create an environment for enantioselective catalysis.[13] However, the major drawback to this approach has been the suitability of the support with an appropriate structure and composition to keep the encapsulated metal phthalocyanine stable and active with the required selectivity.[14] In addition, the requirement for prior functionalization of the support to anchor the catalytic moieties further complicates the procedure in most cases.

Herein, we demonstrate an approach to fabricate a hybrid system, in which the organic component creates an enzymatic environment for the catalytic reactions, while the nanostructured inorganic materials provide the appropriate textural property and structural stability (Scheme 1). The inorganic support can also be seen as a protective structure around the active center of the catalyst, which is similar to the protein mantle that surrounds the active site of enzymes. Our method involves an assembly process similar to that known for bio-silicification in algae, such as diatoms. Polyamines, which are known to be responsible for silicification and the assembly of silica, are used as the organic component to interact with multivalent ions to form supramolecular aggregates in this bioin-

[a] J. Manna, A. J. Amali, Dr. R. K. Rana
Nanomaterials Laboratory, I&PC Division
CSIR-Indian Institute of Chemical Technology
Hyderabad 500007 (India)
Fax: (+91) 40-27160921
E-mail: rkrana@iict.res.in

Supporting information for this article is available on the WWW under http://dx.doi.org/10.1002/chem.201402614.

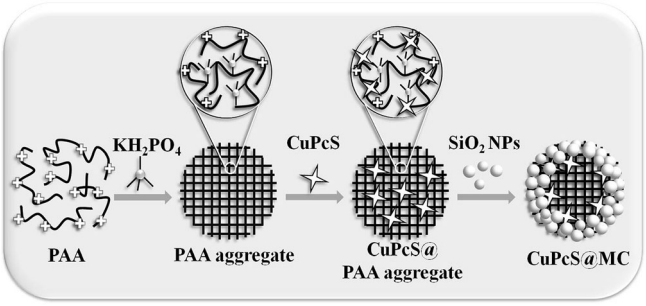

Scheme 1. Schematic representation of the polyamine-mediated assembly to encapsulate CuPcS in the microcapsule (CuPcS@MC).

spired method.[15] These aggregates help to entrap the metal complex and template the silica nanoparticle (NP) assembly, thus generating hybrid microcapsule structures.

Results and Discussion

Typically, the entrapment of a Cu^{II}–phthalocyanine tetrasulphonate (CuPcS) complex in a microcapsule (MC) is carried out by using polyallylamine (PAA) with phosphate ions to form supramolecular PAA aggregates (Scheme 1). Monitoring by dynamic light scattering (DLS) showed that the PAA aggregates were formed with an average size of 332 nm immediately on addition of the phosphate ions to PAA in aqueous solution (see Figure S1 in the Supporting Information). In the second step, the negatively charged CuPcS was chosen to interact with the positively charged ammonium groups of PAA to ensure entrapment in the aggregates. Finally, the assembly of negatively charged silica nanoparticles that are approximately 15 nm in size and surround the CuPcS-containing PAA aggregates form an ordered shell, thus generating the MC structures. Accordingly, the average hydrodynamic diameter determined by DLS changed to approximately 509 nm after the addition of CuPcS and the further addition of silica nanoparticles resulted in an average size of approximately 887 nm.

The optical images of the silica-nanoparticle-assembled microcapsules are shown in Figure 1 a, b. The well-dispersed particles suspended in an aqueous suspension, as seen in the images, indicates that the silica nanoparticles are assembled in a controlled manner to generate the submicron-sized structures. SEM analysis clearly illustrates the spherical morphology of the MCs (Figure 1 c, d). The sizes of the MCs, whether prepared with or without CuPcS, are similar with diameters of 400–700 nm. Further analysis by TEM reveals the shell of the MC structure to have a thickness of 100–150 nm. The shell-wall structure of the MCs is in fact made up of the silica nanoparticles with a diameter of approximately 15 nm, which are clearly seen in the TEM image taken at higher magnification (Figure 1 f). It is also evident in the TEM image that the assembly of these nanoparticles leads to the creation of pores in the shell wall of the MC. As estimated from the N_2-sorption studies, the as-synthesized microcapsules had a BET surface area of 272 $m^2 g^{-1}$ and a pore-size distribution centered at 3.6 nm (see Figure S2 in the Supporting Information).

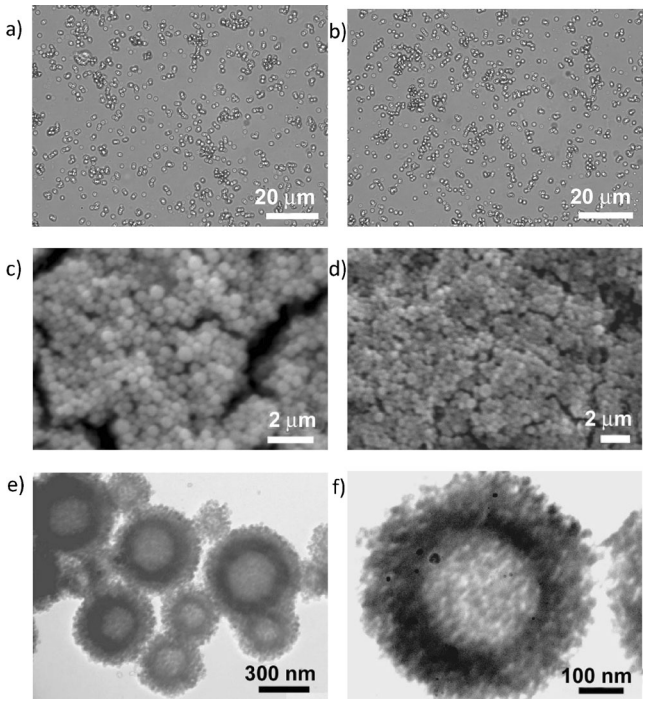

Figure 1. Optical (a, b) and SEM (c, d) images of silica-nanoparticle-assembled microcapsule samples (MC and CuPcS@MC, respectively). TEM (e, f) images of the microcapsules containing CuPcS (CuPcS@MC) at different magnifications.

To locate the presence of CuPcS in the MCs, the CuPcS@MC samples suspended in an aqueous solution were imaged under a confocal microscope. The confocal image showed fluorescence due to the presence of CuPcS (see Figure 2 and Figure S3 in the Supporting Information). The discrete fluorescent spots that emanate from the MCs, as seen from the fluorescence and bright-field images, further signify that the CuPcS molecules are trapped in the microcapsule structure. However, the exact location of the complex could not be ascertained. The spheres are too small for the optical image to distinguish

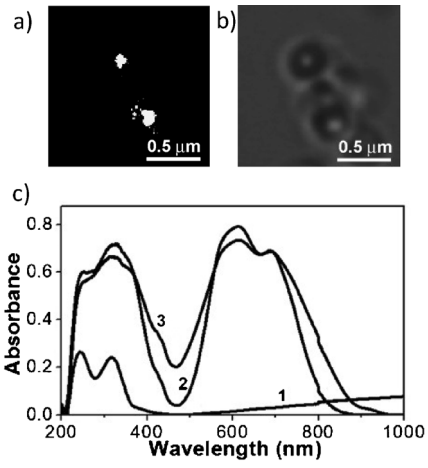

Figure 2. Confocal a) fluorescence and b) bright-field images of CuPcS@MC suspended in an aqueous solution analyzed at $\lambda_{ex} = 633$ nm. c) UV/Vis/DR spectra for the 1) MC, 2) CuPcS@MC, and 3) neat CuPcS.

whether the complexes are in the shell wall or core or are present throughout the structure. As estimated from measurements taken by atomic absorption spectroscopy (AAS), the loading amount of CuPcS in the MCs was 3.05 wt% (Cu ≈0.20 wt%). From thermogravimetric analysis (TGA), we found the total organic content to be 18 wt%, which corresponds to the amount of PAA and CuPcS present in the CuPcS@MC samples (see Figure S4 in the Supporting Information).

The synthesized materials were further characterized by FTIR, micro-Raman, and UV/Vis spectroscopic analysis. In the FTIR spectrum, the vibrational bands at $\tilde{\nu}=1462$ and 1418 cm^{-1} observed in both neat CuPcS and CuPcS@MC samples are attributable to the stretching modes of C=N and C=C of the phthalocyanine ring, respectively (see Figure S5 in the Supporting Information).[16] The confocal micro-Raman spectra of neat CuPcS and CuPcS@MC display a typical intense band at $\tilde{\nu}=1525$ cm^{-1}, which is assignable to a C_β–C_β vibration in phthalocyanine (see Figure S6 and Table S1 in the Supporting Information).[17] The Raman signal at $\tilde{\nu}=1441$ cm^{-1} represents the C–N and C–C of pyrrole moiety of the phthalocyanine unit.

The UV/Vis diffusion reflectance spectra of solid samples of MC, CuPcS@MC, and neat CuPcS are shown in Figure 2b. Phthalocyanine complexes exhibit characteristic Q bands in the visible region due to $\pi\rightarrow\pi^*$ transitions from HOMO–LUMO and B bands (Soret band) in the UV region due to deeper $\pi\rightarrow$ LUMO transitions.[18] The position and splitting of the Q bands are generally assigned to monomeric and dimeric/oligomeric forms.[19] Although the monomeric form absorbs at around $\lambda=$ 700 nm, this band blue-shifts with di-/oligomerization. The neat CuPcS has Q bands centered at $\lambda=689$ and 614 nm. The encapsulated CuPcS in the MCs also exhibited two Q bands at $\lambda=687$ and 612 nm, thus indicating the presence of both mono- and oligomeric forms of the complex in the MCs. The CuPcS@MC also has B bands centered at $\lambda=328$ and 420 nm. Moreover, the similarity in the absorption positions for both the encapsulated CuPcS and neat sample suggests that encapsulation by interaction with polyamine does not perturb the phthalocyanine π system.

We examined the catalytic activity of CuPcS@MCs in epoxidation reactions. Table 1 shows the catalytic performance of CuPcS@MC for the epoxidation of *trans*-stilbene carried out in different solvents at two temperatures. The GC and GC-MS results show that *trans*-stilbene oxide is the only product selectively formed in the reaction carried out at both temperatures. The solvent effect in terms of conversion of *trans*-stilbene follows the order chloroform > DMF > *o*-xylene > *n*-propanol. The solvent polarity is not clearly reflected in the trend of *trans*-stilbene conversion. A highly polar solvent competes with the reactant to interact with the hydrophilic silica surface of the catalyst, thereby resulting in lower conversion of *trans*-stilbene. On the other hand, the least polar solvents allow better solubility of the reactant, but the interaction of the reactant with the catalyst surface is diminished. Hence, medium polar solvents were optimum for higher conversion.

Table 1. Epoxidation of *trans*-stilbene in different solvents.[a]

Entry	Solvent	Conversion [%][b]	
		70 °C	90 °C
1	DMF	20	39
2	$CHCl_3$	50	87
3	*o*-xylene	10	14
4	*n*-propanol	<1	<1

[a] Reactions were carried out with a solvent (5 mL), *trans*-stilbene (0.5 mmol), CuPcS@MC catalyst (5 mg), Na_2CO_3 (1.5 mmol), and TBHP (1.5 mmol) in water (70%) for 24 h. [b] GC conversion.

On the other hand, the blank reaction without the catalyst under similar conditions showed a conversion of 2.3% only (see Table S2 in the Supporting Information). The MCs without CuPcS did not show any appreciable activity either, thus indicating that the encapsulated CuPcS as present in CuPcS@MC are not only accessible to the reactants for reaction, but are also responsible for the observed catalytic activities in the epoxidation of *trans*-stilbene. Interestingly, when we used an equivalent amount of neat CuPcS as in CuPcS@MC as a catalyst under similar conditions, the conversion was only 7% (see Table S2 in the Supporting Information). This outcome clearly suggests that the microcapsule structure offers a suitable environment for better dispersity of CuPcS. Moreover, it is well recognized that the spatial confinement of catalytic systems in appropriate matrices can lead to enhancement of catalytic activity.[20]

The surrounding environment of the phthalocyanine complexes are known to influence their monomeric and oligomeric forms.[19] Although the monomeric forms have been reported to be the active species in catalytic reactions, these complexes often tend to dimerize/oligomerize, thereby resulting in decreased activities.[8a,21] We further analyzed the UV/Vis spectra of the catalyst and the neat complex (see Figure S7a,b in the Supporting Information). From the corresponding deconvoluted spectra, it can be seen that ratio *R* (ratio of the absorbance due to monomeric and oligomeric CuPcS species) in the CuPcS@MC moiety is higher than that in neat CuPcS. Moreover, the interaction of CuPcS with polyamine aggregates as monitored during the microcapsule assembly process also shows stabilization of the monomeric CuPcS species (see Figure S7c in the Supporting Information). Thus, the higher amount of monomeric form in the microcapsules indicates that the ionic interaction amongst CuPcS and the embedded polyamines with the assembled silica nanoparticles in the microcapsule structure allows separation of the oligomerized forms of the complex. It is also known that heating of phthalocyanine can lead to stabilization of the monomeric form.[22] Therefore, we further examined the possibility of increasing the monomeric form by heating the catalysts at various temperatures. As observed from our experiments, the *R* ratio is increased with an increase in the heating temperature (see Figure S7d,e in the Supporting Information). When the heat-treated CuPcS@MC catalysts were used in the epoxidation reaction, the activities increased to conversions of 60 and 65%, respectively. This outcome further supports the observed enhancement in activity

for the encapsulated CuPcS relative to the neat sample and justifies the importance of monomeric species in the reaction.

We used various other oxidants in the catalytic reaction (see Table S3 in the Supporting Information). *tert*-Butyl hydroperoxide (TBHP) in decane showed a lesser activity than TBHP in water, whereas only traces of the conversion products were observed with oxygen or H_2O_2 as the oxidant. Decane, a nonpolar solvent, restricts the surface interaction of the reactants as discussed earlier, thereby decreasing the catalytic activity. The catalytic activity of CuPcS@MC was checked for the epoxidation of various other cyclic and open-chain alkenes as the oxidant at 70 °C (the results are summarized in Table 2). The catalyst exhibits good conversion with the epoxide as the only product, except for cyclohexene (see Figures S8 and S9 in the Supporting Information). As reported earlier, cyclohexene can undergo allylic oxidation to produce 2-cyclohexene-1-one as the other product.[23]

Table 2. Oxidation of various alkenes.[a]

Entry	Substrate	Conversion [%][b]
1	stilbene	50
2	styrene	50
3	cyclooctene	37
4	cyclohexene	38[c]
5	1-decene	14

[a] Reactions were carried out with a solvent (5 mL), *trans*-stilbene (0.5 mmol), CuPcS@MC catalyst (5 mg), Na_2CO_3 (1.5 mmol), and TBHP (1.5 mmol) in water (70%) for 24 h. [b] GC conversion. [c] Conversion was 21 and 17% for the formation of the epoxide and 2-cyclohexene-1-one, respectively.

To check the reusability of the catalyst, the CuPcS@MC catalyst was collected by centrifugation after the first reaction cycle, washed with $CHCl_3$ and water, and dried. The catalyst was reused several times for the oxidation of *trans*-stilbene in $CHCl_3$ at 70 and 90 °C (Figure 3 a). The catalytic activity remains almost similar for all the cycles tested. Analysis by AAS of the reaction mixture showed that there was no leaching of CuPcS during the reaction. UV/Vis/DRS analysis of the reused CuPcS@MC catalyst after different cycles shows unaltered signatures of the CuPcS entrapped in the microcapsule structure (Figure 3 b). Although there was little agglomeration in the sample of the used catalyst, it did not affect the epoxidation reaction, thus indicating the stability of the active monomeric species (see Figure S10 in the Supporting Information).

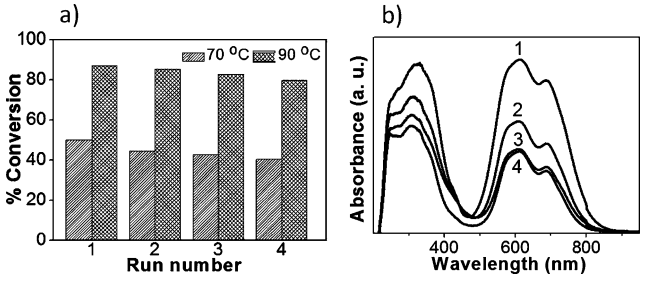

Figure 3. a) Catalytic activity of the reused CuPcS@MC catalyst at different reaction cycles for the epoxidation of *trans*-stilbene and b) UV/Vis/DLS of the used catalyst CuPcS@MC after cycles 1–4 (1)–(4), respectively, at 90 °C.

Conclusion

We have demonstrated a facile and efficient bioinspired approach to encapsulate a copper–phthalocyanine complex in silica-nanoparticle-assembled microcapsules. The presence of a polyamine not only allowed encapsulation of the CuPcS during the catalyst preparation, but also aided the stabilization of the monomeric forms of the complex, as required for catalytic activity. On the other hand, the surrounding silica nanoparticles provided structural stability towards any leaching of the complex. Therefore, we anticipate that this approach may further expand the scope of investigations of various other active metal centers, which may aid the design of new bioinspired catalysts with possible uses as diverse substrates and tune selectivity.

Experimental Section

Materials

Potassium dihydrogen phosphate (KH_2PO_4), polyallylamine (17 kDa), Cu^{II}–phthalocyanine tetrasulphonic acid tetrasodium salt (CuPcS), colloidal silica nanoparticles (Ludox HS-40, average particle diameter ≈ 13 nm, 40 wt%), *trans*-stilbene, cyclohexene, cyclooctene, styrene, TBHP, and hydrogen peroxide were procured from Sigma–Aldrich and used as received. In all cases, Millipore water (18.2 MΩ) was used to prepare the solutions.

Synthesis of CuPcS@MCs

In a typical process, polyallylamine (1.68 mL, 2 mg mL^{-1}, 17 kDa; 1 Da = 1 g mol^{-1}) was vortex mixed with an aqueous solution of KH_2PO_4 (0.01 M, 10 mL) at a speed 4–5 for 10 s. The slightly cloudy suspension of PAA PO_4 aggregates was aged for 1 min and then mixed with an aqueous solution of CuPcS (0.6 mM, 0.8 mL) for 10 s. After ageing the resulting bluish suspension for 10 min, colloidal silica (10 mL) was added and vortex mixed for 20 s to form the microcapsules. The final bluish suspension was allowed to age for 3 h, centrifuged (7000 rpm, 2 min), and washed three times with water. The light-blue precipitate of CuPcS@MC was dried at room temperature and used for further characterization and catalytic reactions.

Catalytic epoxidation reactions

In a typical reaction, *trans*-stilbene (0.5 mmol) was dissolved in $CHCl_3$ (5 mL) with the catalyst (5 mg), sodium carbonate (1.5 mmol), and TBHP (1.5 mmol, 70 wt%) in a 50 mL closed container (autoclave). The reaction was carried out at the required temperature and monitored by GC on a ZB-5 column. After the reaction, the catalyst CuPcS@MC was separated from the reaction mixture by centrifugation (7000 rpm, 2 min) and washed with $CHCl_3$ and water to be reused in the next reaction.

Acknowledgements

Financial support from DST India (SR/NM/NS-111/2010) and CSIR India (IntelCoat, NanoSHE, and SRF) are acknowledged. We thank Dr. S.V. Manorama, Dr. R.K. Banerjee, Dr. K. V.S.N. Raju, and A. Kumar for their help with the characterization of the materials.

Keywords: epoxidation · heterogeneous catalysis · nanostructures · phthalocyanine · self-assembly

[1] a) L. Que, W. B. Tollman, *Nature* **2008**, *455*, 333 – 340; b) S. R. Lewis, S. Dutta, M. H. Gui, E. L. Coker, F. E. Huggins, S. Daunert, L. Bacgas, D. Bhattacharyya, *Proc. Natl. Acad. Sci. USA* **2011**, *108*, 8577 – 8582.

[2] a) D. den Boer, M. Li, T. Habets, P. Iavicoli, A. E. Rowan, R. J. M. Nolte, S. Speller, D. B. Amabilino, S. De Feyter, J. A. A. W. Elemans, *Nat. Chem.* **2013**, *5*, 621 – 627; b) R. Latifi, J. S. Valentine, W. Nam, S. P. de Visser, *Chem. Commun.* **2012**, *48*, 3491 – 3493; c) W. L. Man, W. W. Y. Lam, H. K. Kwong, S. M. Yio, T. C. Lau, *Angew. Chem.* **2012**, *124*, 9235 – 9238; *Angew. Chem. Int. Ed.* **2012**, *51*, 9101 – 9104.

[3] a) I. G. Denisov, T. M. Makris, S. G. Sligar, I. Schlichting, *Chem. Rev.* **2005**, *105*, 2253 – 2278; b) J. H. Dawson, *Science* **1988**, *240*, 433 – 439.

[4] a) M. Orio, O. Jarjayes, H. Kanso, C. Philouze, F. Neese, F. Thomas, *Angew. Chem.* **2010**, *122*, 5109 – 5112; *Angew. Chem. Int. Ed.* **2010**, *49*, 4989 – 4992; *Angew. Chem.* **2010**, *122*, 5109 – 5112; b) K. J. Humphreys, L. M. Mirica, Y. Wang, J. P. Klinman, *J. Am. Chem. Soc.* **2009**, *131*, 4657 – 4663; c) E. I. Solomon, P. Chen, M. Metz, S.-K. Lee, A. E. Palmer, *Angew. Chem. Int. Ed.* **2001**, *40*, 4570 – 4590; *Angew. Chem.* **2001**, *113*, 4702 – 4724.

[5] A. B. Sorokin, *Chem. Rev.* **2013**, *113*, 8152 – 8191.

[6] R. F. Parton, I. Vankelecom, C. P. Bezoukhanova, M. Casselman, J. Uytterhoeven, P. A. Jacobs, *Nature* **1994**, *370*, 541 – 544.

[7] S. Seelan, A. K. Sinha, D. Srinivas, S. Sivasanker, *J. Mol. Catal. A* **2000**, *157*, 163.

[8] a) R. F. Parton, P. E. Neys, P. A. Jacobs, R. C. Sosa, P. G. Rouxhet, *J. Catal.* **1996**, *164*, 341; b) A. B. Sorokin, P. Buisson, A. C. Pierre, *Microporous Mesoporous Mater.* **2001**, *46*, 87.

[9] Y. Tanamura, T. Uchida, N. Teramae, M. Kikuchi, K. Kusaba, Y. Onodera, *Nano Lett.* **2001**, *1*, 387.

[10] S. V. Sirotin, A. Y. Tolbin, I. F. Moskovskaya, S. S. Abramchuk, L. G. Tomilova, B. V. Romanovsky, *J. Mol. Catal. A* **2010**, *319*, 39.

[11] a) M. Pirouzmand, M. M. Amini, N. Safari, *J. Colloid Interface Sci.* **2008**, *319*, 199 – 205; b) M. Alvaro, E. Carbonell, M. Espla, H. Garcia, *Appl. Catal. B* **2005**, *57*, 37 – 42.

[12] a) A. Hirth, A. K. Sobbi, D. Wöhrle, *J. Porphyrins Phthalocyanines* **1997**, *1*, 275; b) M. Sánchez, N. Chap, J.-B. Cazaux, B. Meunier, *Eur. J. Inorg. Chem.* **2001**, *7*, 1775.

[13] M. T. Reetz, N. Jiao, *Angew. Chem.* **2006**, *118*, 2476 – 2479; *Angew. Chem. Int. Ed.* **2006**, *45*, 2416 – 2419; *Angew. Chem.* **2006**, *118*, 2476 – 2479.

[14] B. M. L. Dioos, I. F. J. Vankelecom, P. A. Jacobs, *Adv. Synth. Catal.* **2006**, *348*, 1413 – 1446.

[15] a) G. Begum, R. K. Rana, S. Shing, L. Satyanarayana, *Chem. Mater.* **2010**, *22*, 551 – 556; b) R. K. Rana, V. S. Murthy, J. Yu, M. S. Wong, *Adv. Mater.* **2005**, *17*, 1145 – 1150; c) A. J. Amali, P. Saravanan, R. K. Rana, *Angew. Chem.* **2011**, *123*, 1354 – 1357; *Angew. Chem. Int. Ed.* **2011**, *50*, 1318 – 1321; *Angew. Chem.* **2011**, *123*, 1354 – 1357.

[16] a) M. Fukui, N. Katayama, Y. Ozaki, T. Araki, K. Iriyama, *Chem. Phys. Lett.* **1991**, *177*, 247; b) J. Dowdy, J. J. Hoagland, K. W. Hipps, *J. Phys. Chem.* **1991**, *95*, 3751.

[17] a) B. J. Palys, D. M. W. van dem Ham, W. Briels, D. Feil, *J. Raman Spectrosc.* **1995**, *26*, 63 – 76; b) T. V. Basova, B. A. Kolesov, *J. Struct. Chem.* **2000**, *41*, 770 – 777.

[18] a) M. Sommeraurer, C. Rager, M. Hanack, *J. Am. Chem. Soc.* **1996**, *118*, 10085 – 10095; b) S. U. Lee, J. C. Kim, H. Mizuseki, Y. Kawazoe, *Chem. Asian J.* **2010**, *5*, 169.

[19] K. Kervinen, P. C. A. Bruijnincx, A. M. Beale, J. G. Mesu, G. V. Koten, R. J. M. K. Gebbink, B. M. Weckhuysen, *J. Am. Chem. Soc.* **2006**, *128*, 3208 – 3217.

[20] a) A. M. Yashchenok, M. Delcea, K. Videnova, E. A. Jares-Erijman, T. M. Jovin, M. Konrad, H. Mohwald, A. G. Skirtach, *Angew. Chem.* **2010**, *122*, 8293 – 8297; *Angew. Chem. Int. Ed.* **2010**, *49*, 8116 – 8120; b) J. E. Yoo, K. Lee, M. Altomare, E. Selli, P. Schmuki, *Angew. Chem.* **2013**, *125*, 7662 – 7665; *Angew. Chem. Int. Ed.* **2013**, *52*, 7514 – 7517.

[21] a) C. R. Jacob, S. P. Varkey, P. Ratnasamy, *Appl. Catal. A* **1998**, *168*, 353 – 364; b) B. M. Choudary, M. L. Kantam, B. Bharathi, P. Sreekanth, F. Figueras, *J. Mol. Catal. A* **2000**, *159*, 417 – 421.

[22] P. D. Fuqua, B. Dunn, *J. Sol-gel sci. Technol.* **1998**, *11*, 241 – 250.

[23] L. M. González, A. L. Villa de P., C. Montes de C., A. Sorokin, *Tetrahedron Lett.* **2006**, *47*, 6465 – 6468.

Received: March 31, 2014
Published online on June 2, 2014